RECENT PROGRESS IN L-H TRANSITION STUDIES AT JET: TRITIUM, HELIUM, HYDROGEN AND DEUTERIUM

E.R. Solano[1], E. Delabie[2], G. Birkenmeier[3,4], C. Silva[5], J.C. Hillesheim[6], P. Vincenzi[7], A.H. Nielsen[8], J.Juul Rasmussen[8], A. Baciero[1], S. Aleiferis[6,9], I. Balboa[6], A. Boboc[6], C. Bourdelle[10], I.S. Carvalho[5], P. Carvalho[5], M.ºChernyshova[11], R. Coelho[5], T. Craciunescu[12], R. Dumont[10], P. Dumortier[18], E. de la Luna[1], J. Flanagan[6], M. Fontana[6], J.M.ºFontdecaba[1], L. Frassinetti[14], D. Gallart[15], J. Garcia[10], E. Giovannozzi[16], C. Giroud[6], W.Gromelski[11], R.Henriques[5], L. Horvath[6], P. Jacquet[6], I. Jepu[12], A. Kappatou[4], D.L. Keeling[6], D. King[6], E. Kowalska-Strzęciwilk[11], M.Lennholm[17], E. Lerche[18], E. Litherland-Smith[6], V. Kiptily[6], K. Kirov[6], A. Loarte[19], B. Lomanowski[20], C.F.ºMaggi[6], M.J. Mantsinen[21], A. Manzanares[22], M. Maslov[6], A.G. Meigs[6], I. Monakhov[6], R.B. Morales[6], D. Nina[5], C.ºNoble[6], V. Parail[6], F. Parra Diaz[23], E. Pawelec[24], G. Pucella[16], D. Réfy[25], E. Righi-Steele[17], F.G. Rimini[6], T.ºRobinson[6], S. Saarelma[6], M. Sertoli[6], A. Shaw[6], S. Silburn[6], P. Sirén[6], Ž. Štancar[26], H. Sun[6], G. Szepesi[6], D. Taylor[6], E.ºTholerus[14], S.ºVartanian[10], G. Verdoolaege[27], B. Viola[16], H. Weisen[13] and T. Wilson[6] and JET Contributors *

[1]Laboratorio Nacional de Fusión, CIEMAT, Madrid, Spain; [2]Oak Ridge National Laboratory, Oak Ridge, TN 37831-6169, TN, United States of America; [3]Physik-Department E28, Technische Universität München, 85748 Garching, Germany; [4]Max-Planck-Institut für Plasmaphysik, D-85748 Garching, Germany; [5]Instituto de Plasmas e Fusão Nuclear, Instituto Superior Técnico, Universidade de Lisboa, Portugal; [6]CCFE, Culham Science Centre, Abingdon, Oxon, OX14 3DB, United Kingdom of Great Britain and Northern Ireland; [7]Consorzio RFX, Corso Stati Uniti 4, 35127 Padova, Italy; [8]Department of Physics, Technical University of Denmark, Bldg 309, DK-2800 Kgs Lyngby, Denmark; [9]NCSR 'Demokritos' 153 10, Agia Paraskevi Attikis, Greece; [10]CEA, IRFM, F-13108 Saint Paul Lez Durance, France; [11]Institute of Plasma Physics and Laser Microfusion, Hery 23, 01-497 Warsaw, Poland; [12]The National Institute for Laser, Plasma and Radiation Physics, Magurele-Bucharest, Romania; [13]Ecole Polytechnique Fédérale de Lausanne (EPFL), Swiss Plasma Center (SPC), CH-1015 Lausanne, Switzerland; [14]Fusion Plasma Physics, EES, KTH, SE-10044 Stockholm, Sweden; [15]Barcelona Supercomputing Center, Barcelona, Spain; [16]Unità Tecnica Fusione, ENEA C. R. Frascati, via E. Fermi 45, 00044 Frascati (Roma), Italy; [17]European Commission, B-1049 Brussels, Belgium; [18]Laboratory for Plasma Physics Koninklijke Militaire School, Ecole Royale Militaire Renaissancelaan 30 Avenue de la Renaissance B-1000, Brussels, Belgium; [19]ITER Organization, Route de Vinon, CS 90 046, 13067 Saint Paul Lez Durance, France; [20]Aalto University, PO Box 14100, FIN-00076 Aalto, Finland; [21]ICREA and Barcelona Supercomputing Center, Barcelona, Spain; [22]Universidad Complutense de Madrid, Madrid, Spain; [23]Rudolf Peierls Centre for Theoretical Physics, University of Oxford, Oxford OX1 3PU, United Kingdom of Great Britain and Northern Ireland; [24]Institute of Physics, Opole University, Oleska 48, 45-052 Opole, Poland; [25]Centre for Energy Research, Budapest, Hungary; [26]Slovenian Fusion Association (SFA), Jozef Stefan Institute, Jamova 39, SI-1000 Ljubljana, Slovenia; [27]Department of Applied Physics, UG (Ghent University), St-Pietersnieuwstraat 41 B-9000 Ghent, Belgium

* See the author list of 'Overview of JET results for optimising ITER operation' by J. Mailloux et al to be published in Nuclear Fusion Special issue: Overview and Summary Papers from the 28th Fusion Energy Conference (Nice, France, 10-15 May 2021)

*NF_IAEA_2021_Solano_R4.docx

Abstract

We present an overview of results from a series of L-H transition experiments undertaken at JET since the installation of the ITER-like-wall (JET-ILW), with Beryllium wall tiles and a Tungsten divertor. Tritium, Helium and Deuterium plasmas have been investigated. Initial results in Tritium show ohmic L-H transitions at low density and the power threshold for the L-H transition (P_{LH}) is lower in Tritium plasmas than in Deuterium ones at low densities, while we still lack contrasted data to provide a scaling at high densities. In Helium plasmas there is a notable shift of the density at which the power threshold is minimum ($\bar{n}_{e,min}$) to higher values relative to Deuterium and Hydrogen references. Above $\bar{n}_{e,min}$ (He) the L-H power threshold at high densities is similar for D and He plasmas. Transport modelling in slab geometry shows that in Helium neoclassical transport competes with interchange-driven transport, unlike in Hydrogen isotopes. Measurements of the radial electric field in Deuterium plasmas show that E_r shear is not a good indicator of proximity to the L-H transition. Transport analysis of ion heat flux in Deuterium plasmas show a non-linearity as density is decreased below $\bar{n}_{e,min}$. Lastly, a regression of the JET-ILW Deuterium data is compared to the 2008 ITPA scaling law.

1. INTRODUCTION

Characterizing and understanding the power threshold conditions for ITER to achieve H-modes (P_{LH}) is a major goal of a series of L-H transition experiments undertaken at JET since the installation of the ITER-like-wall (JET-ILW), with Beryllium wall tiles and Tungsten divertor [1-4]. In JET it has been shown [1, 2] that the metal wall affects the L-H transition power thresholds. In consequence here we report only on JET-ILW L-H transition experiments, with slow power ramps, of order ~1 MW/s. As usual, the L-H transition power threshold, P_{LH}, is measured either as $P_{loss} = P_{Ohm} + P_{Aux} - dW/dt$ or as $P_{sep} = P_{loss} - P_{rad,bulk}$. For fixed shape, current and toroidal field, it is conventional to display plots of P_{loss} or P_{sep} as a function of electron line-averaged density, $\bar{n}_e$, to identify the density at which the power threshold is minimum, $\bar{n}_{e,min}$. It is also conventional to label L-H transitions as taking place in the high or low density branch accordingly. High density branch data, with $n_e > \bar{n}_{e,min}$, was used to build the multi-machine ITPA 2008 L-H transition power threshold scaling [5], often displayed with threshold data for reference.

Fig. 1: typical plasma shapes at JET: a) CC, Corner, b) VT, Vertical Target and c) HT, Horizontal Target.

The effect of strike line location on the L-H power threshold is very strong in JET-ILW [1]. All plasmas discussed in detail in this manuscript have the same shape, HT shown in Fig. 1c, with the inner strike line on the vertical target and the outer strike line on a tilted target. Other shapes shown in Fig. 1 will be discussed only in section 4.3, showing the influence of plasma shape on power threshold scaling.

In this contribution, we present a progress report on results from L-H transitions studies in Tritium in section 2 (preliminary, data points in plots in magenta), and in [4]Helium (data-points in plots in green), Deuterium (data-points in plots in blue) and matching Hydrogen (Proteum) plasmas (data points in red) in Section 3 [6]. We include a brief study of ELMy H-mode in Helium, the regime in which ELM mitigation and control will need to be tested in ITER.

We also present results from recent Deuterium L-H transition studies. An upgraded Doppler reflectometry diagnostic enabled measurement of fluctuation velocities in the plasma edge region, revealing that in fact there is no noticeable evolution of the radial electric field along the power ramp, shown in Section 4.1 [7]. We infer that shear of time-averaged perpendicular fluctuation velocity or radial electric field is unlikely to control the transition. A study of the ion heat flux at the transition time as a function of target plasma density in Deuterium plasmas is presented in section 4.2. In section 4.3 we present an update the JET L-H power threshold scaling. Summary and discussions are presented in Section 5.

Our intention is to highlight recent studies and results at JET, rather than to present an extensive overview of L-H transition studies.
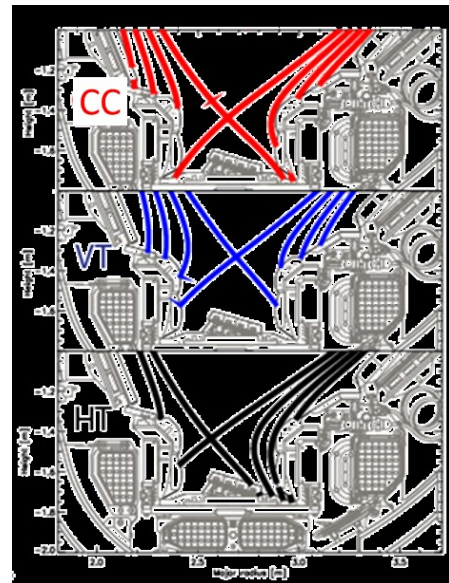
Recent progress in L–H transition studies at JET in tritium, helium, hydrogen and deuterium

[Left hand page running head is author's name in Times New Roman 8 point bold capitals, centred. For more than two authors, write AUTHOR et al.]

2.   PRELIMINARY RESULTS FROM L-H TRANSITION STUDIES IN TRITIUM PLASMAS

L-H transition studies in Tritium were performed in plasmas with B_{tor}=1.8 T, I_p=1.7 MA, HT shape, to be compared with the available Deuterium P_{LH} matching dataset, described in more detail later.

In December 2020, while waiting for the Neutral Beam Injection (NBI) system to change-over from Deuterium (D) to Tritium (T), and after a few Hydrogen (Protium, H) plasmas, we had the opportunity to investigate L-H transitions in plasmas with varying mixtures of Hydrogen and Tritium (H+T), and in Tritium plasmas. We reported on the RF Tritium L-H studies in the proceedings of the IAEA FEC 2021 conference [8], with the puzzling result that the L-H threshold power was higher in T than in D. Since then we have found that the phase control of the RF wave launched in those plasmas was inadequate. This affects the evaluation of the power delivered to the plasma, and may also explain in part the increased radiation observed since part of the RF power possibly interacts directly with the wall. Those results are presently being revised and will be reported in a forthcoming publication.

Shown in Fig. 2, on the left, are two ohmic L-H transitions observed in a Tritium plasma. No auxiliary power is applied, and during this phase of the pulse, the density is feedback-controlled. At 6.55 s the plasma spontaneously enters H-mode, as evidenced by the increase in pedestal density and the appearance of an M-mode [9], evident in divertor magnetics as an n=0, in ECE edge channels and in divertor T_{alpha} signals. The gas is reduced by the feedback system and this leads to a density drop and a back-transition into L-mode at 8.7 s, soon followed by another brief L-H and H-L phases. We observed quite a few transient ohmic H-modes in various Tritium pulses. On the right, we show L-H transitions during a Tritium-NBI power ramp later in the same pulse. The second transition is discarded as an accurate measurement of the power threshold because of the large transient peak in the radiated power just before the transition.

In Fig. 3 we show P_{loss} and P_{sep} as a function of $\bar{n}_e$ for Deuterium and Tritium plasmas. The ohmic transitions, marked with *, indicate that in Tritium $\bar{n}_{e,min}$ is lower than in Deuterium, as expected from the experimental fact that $\bar{n}_{e,min}$ is higher in Hydrogen than in Deuterium (shown below, in Fig. 4). The NBI data point indicates that the power threshold in Tritium is somewhat lower than in Deuterium as well, but no isotope scaling of the power threshold can be attempted yet. Further L-H transition experiments in Tritium are planned for early 2022. We also plot in figure 3 the corresponding ITPA 2008 scaling law for D, marked with a blue dotted line. Assuming that the power threshold scales inversely with isotope mass, we compute the Tritium ITPA scaling, plotted with a magenta dashed line. The ITPA scaling was constructed for P_{loss} values, typically in situations with low P_{rad}. Since high P_{rad} is unavoidable in many RF-heated plasmas in JET, we compare P_{sep} with the ITPA scaling, following the lead of the ITER team [13], assuming low P_{rad} is to be expected in ITER.
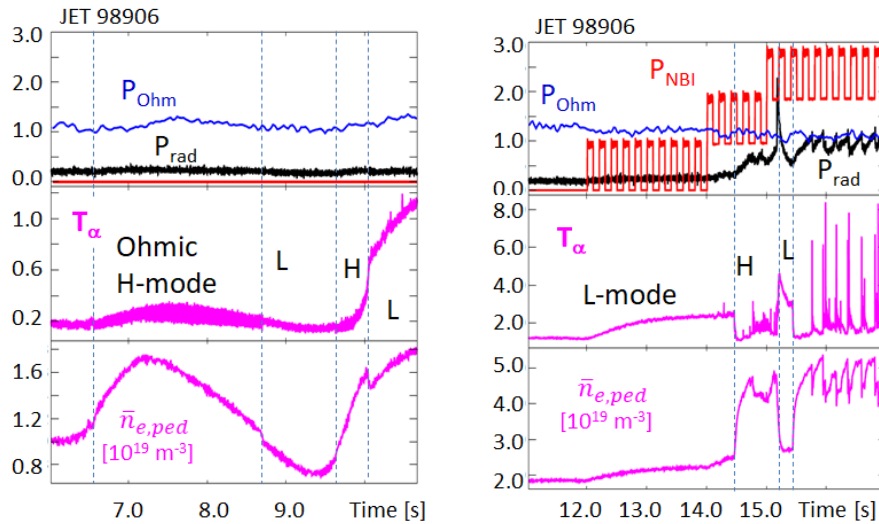

Fig. 2: On the left, ohmic L-H transitions in Tritium, on the right, NBI L-H transitions. : a) NBI and Ohmic power and bulk radiation, P_{rad}; b) T_α from inboard divertor; c) line-integrated pedestal density, measured with a vertical interferometer line that crosses the plasma edge region.
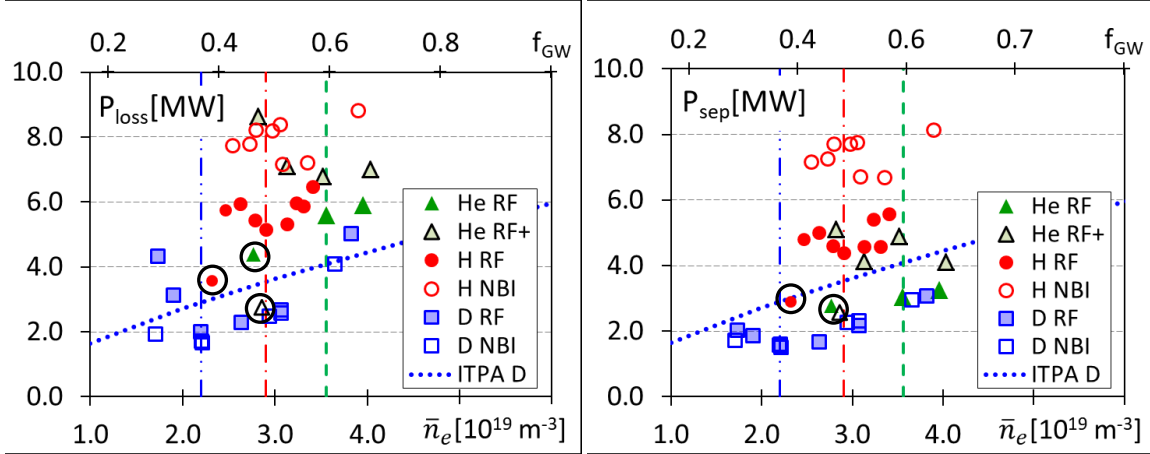
Recent progress in L–H transition studies at JET: tritium, helium, hydrogen and deuterium
FTP/1-4 or similar

[Left hand page running head is author's name in Times New Roman 8 point bold capitals, centred. For more than two authors, write **AUTHOR et al.**]

Fig. 3: a) P_{loss} and b) P_{sep} as a function of line averaged density for Deuterium (blue squares) and Tritium. In Tritium the points marked with an * are ohmic transitions, the circle is quasi-ohmic (0.5 MW of RF, 1.3 MW ohmic), while the diamond has an NBI power ramp. The blue dotted line shows the 2008 ITPA scaling for D, dashed magenta for T.

Measurements of H, D, and T concentration in the JET sub-divertor region are made with an Optical Penning Gauge [10,11]. In all T cases reported here $n_T/n_{H+D+T}>95\%$, and $n_D/n_{H+D+T} <1\%$. In these pulses, **no** D was injected, but trace concentrations of residual D were present. Using a combination of TRANSP modelling [12] and neutron measurements we find that $n_D/n_e<1\%$. At an average neutron rate of approximately $2 \cdot 10^{12}$ s^{-1}, about 75 % of neutrons were calculated to be produced by the T(T,2n)^{4}He reaction, with the remainder stemming from DT fusion [13]. Therefore neutron measurements confirm the purity assessment of the spectroscopic measurements for these Tritium plasmas.

3.   L-H TRANSITION AND ELM STUDIES IN HELIUM PLASMAS

The ITER Research Plan includes a Pre-Fusion Operation Power (PFPO) phase with either Hydrogen or Helium (or mixed) plasmas to investigate ELM suppression (at low toroidal field) as early as possible, before the nuclear phase that starts with Deuterium plasmas. We studied the L-H power threshold in ^{4}Helium plasmas in the JET-ILW to compare with Hydrogen and Deuterium plasmas. We present here a summary of a more extended study of L-H transitions in Helium plasmas [6].

To ensure minimal contamination of the Helium plasmas in this study, we took advantage of 18 calibration pulses taken with only Helium gas injection (no injection of Hydrogenic species). These pulses, unrelated to our experiments, ensured Helium purity before we started our Helium experiments: they had $Z_{eff}=2\pm0.05$. Throughout the calibration pulses and the L-H transition pulses, the divertor cryopump operated as usual, removing Hydrogenic species. No Argon frosting was used to pump Helium. For RF heating the H concentration n_H/n_e was kept below 5%. Spectroscopic measurements of ^{4}He concentration show that in all cases the L-H transition happens with Helium concentration $n_{He}/n_e> 0.48$, and corresponding Helium fraction $n_{He}/(n_{He}+n_H+n_D)> 0.92$.

3.1. L-H transition power threshold in Helium, Hydrogen, Deuterium

A prediction for the L-H power threshold in ITER in Helium plasmas was made inspired by the AUG observation that in their electron heated plasmas a sufficient edge ion heat flux is necessary to achieve a sufficient radial electric field (shear) for the transition to take place [14]. Assuming pure electron heating in ITER, $\bar{n}_{e,min}$ has been evaluated based on 1.5-D transport modelling as the density at which the ratio of edge ion power flux to total edge power flux starts to saturate with increasing electron density (line-averaged). The result of this modelling is the prediction that in ITER $\bar{n}_{e,min}\sim0.4\times n_{e,GW}$ for $q_{95}= 3$ and it is almost independent of the ion species, (D, H or He) [15]. The transition condition in that model is itself based on the assumption that the Helium power threshold, P_{LH}(He), is $1.4\times P_{LH}$(D), while P_{LH}(H)=$2\times P_{LH}$(D), a result from earlier JET-C L-H transition studies [16].

In our recent L-H transition studies in Helium at JET, the ICRH (H minority heating) power ramps reached a flat-top and were then augmented by D-NBI blips (50 ms at 1.3 MW, followed by 50 ms at 2.7 MW of NBI, added to the stationary ICRH power reached in each pulse). The blips were added 450 ms after the RF power had reached its maximum value, both to increase the total auxiliary power and to enable CX measurements of T_i.

Recent progress in L–H transition studies at JET: tritium, helium, hydrogen and deuterium
[Left hand page running head is author's name in Times New Roman 8 point bold capitals, centred. For more than two authors, write
AUTHOR et al.]

Fig. 4a) P_{loss} *and 4b)* P_{sep} *at the L-H transition as a function of line averaged density (lower horizontal axis) and fraction of Greenwald density* f_{GW} *(upper horizontal axis) for Hydrogen, Deuterium and Helium 1.7 MA HT plasmas. The dark Helium symbols correspond to pure ICRH, lighter ones with black boundary have added NBI blips. The datapoints circled in black have lower plasma current and correspondingly lower power threshold. Vertical lines indicate* $\bar{n}_{e,min}$ *and respective* f_{GW} *for each species: blue for D, red for H, green for He. Dotted blue line indicates 2008 ITPA Deuterium scaling law.*

Conventionally, P_{loss} at JET is computed smoothing the input power, the ohmic power, the plasma energy and its time derivative dW/dt, with a smoothing window of 235 ms, and the values are averaged 70 ms before the L-H transition, to avoid using values affected by the post-transition conditions. But because most of the L-H transitions observed in the RF-heated Helium plasmas actually took place during the short-lived additional NBI blips we evaluate P_{loss} and P_{sep} for those cases with only 30 ms smoothing.

Shown in Fig. 4a is P_{loss} at the L-H transition as a function of density for Hydrogen, Deuterium and Helium in 1.8 T, (mostly) 1.7 MA HT plasmas, while Fig. 4b shows the corresponding P_{sep} values. The H and He datapoints surrounded by black circles correspond to lower plasma currents, they are discussed later in this section and in section 3.3, the reader should ignore them for now. The horizontal axis along the top labels the Greenwald fraction f_{GW} (the ratio of average plasma density to the Greenwald limit density) for the 1.7 MA plasma current. The Helium data points in dark green reflect pure RF heating, while the He triangles filled in light green with black outline correspond to transitions during the added NBI blips. The transitions during the NBI blips are necessarily brief, and yet more power may be necessary for a transition to steady H-mode.

We see in Figs 4a and 4b that the density at which P_{LH} is minimum, $\bar{n}_{e,min}$, is considerably higher for Helium than for Deuterium, and somewhat higher than for Hydrogen. In terms of the Greenwald limit density, $\bar{n}_{e,min}(D)$ ~0.4×n_{GW}, $\bar{n}_{e,min}(H)$~0.5×n_{GW}, $\bar{n}_{e,min}(He)$~0.6×n_{GW} for the 1.7 MA dataset. The shift in $\bar{n}_{e,min}$ is clearer in P_{loss}, Fig. 4a, but can still be seen in P_{sep}, Fig. 4b. We have found a similar shift in $\bar{n}_{e,min}$ with a different plasma shape (Corner, CC, see Fig. 1) at the same field and current, and at a higher field, with D-NBI heating [6]. In all Helium plasmas, we find that the L-H transition takes place when the outer strike line is attached, even at the highest densities. At the inner strike line, the plasma is partially detached. Note that the difference between P_{loss} and P_{sep} correspond to radiation in the plasma core, inside 0.95. This radiation is considerable in Helium plasmas at JET [6]. As shown in Fig. 4b, above $\bar{n}_{e,min}(He)$, Deuterium and Helium have similar P_{sep}, below the ITPA 2008 scaling. At high-density Hydrogen has much higher P_{loss} and P_{sep}: L-H transitions couldn't be obtained at high density with the available RF heating at JET at the time, 6 MW.

In DIII-D L-H studies of I_p = 1.0 MA, B_T = 1.65 T, q_{95}=4.1 plasmas report a ~20% increase in $\bar{n}_{e,min}$ in Helium, from 0.33×n_{GW} to 0.4×n_{GW} [17] a noticeable change, although lower than the 50% change we report. AUG studies, in mixed currents and fields, show no difference in $\bar{n}_{e,min}$ between H, D and He, and the same P_{LH} for D and He [18]. C-Mod L-H transition data at 5.4T, 0.9 MA, q_{95}~ 3.65-> 3.9 [19] report a 40% shift, from $\bar{n}_{e,min}(D)$ =0.17×n_{GW} to $\bar{n}_{e,min}(He)$=0.24×n_{GW}. It is not understood why AUG is different, but it must be remembered that $\bar{n}_{e,min}$ can depend on plasma shape, current, field, etc… and those dependencies are not understood yet, in any device.

While discussing the comparison of our results from those in other devices we must mention that, since the installation of the ITER-like wall at JET, the intrinsic Carbon content of the plasma has been too low to allow routine charge exchange measurements of Carbon temperature and rotation across the pedestal formation region [20]. Typically Neon is injected to facilitate core CX measurements, but low Z impurities alter the power

5

thresholds [2], so this is avoided in L-H experiments at JET. Additionally in Helium plasmas we lack the calibration necessary to measure edge Doppler shifts, so again we have no edge rotation measurements. Therefore we can't comment on the impact of torque reported in DIII-D [21] and AUG [14], or ion heat flux [22] on the L-H transition power thresholds for NBI *vs.* wave heating in these H or He plasmas in JET.

We must note that no significant differences are observed in the L-H threshold between NBI or RF heated Deuterium plasmas, especially in the high density branch [23]. The notably higher threshold in NBI vs. RF heated Hydrogen plasmas in JET, also displayed in Fig. 3 and discussed in [23], remains unexplained for now.

From the 1.8T, 1.7 MA data set shown we can infer that the potential increase in the predicted P_{sep} for ITER due to higher $\bar{n}_{e,min}$ in He (compared to H and D) is compensated by the lower power required to access it, and in consequence the predicted P_{LH} for ITER remains unchanged. The ITER team had assumed $P_{LH}(He)=1.4 \times P_{LH}(D)$, while our experiments find $P_{LH}(He)=P_{LH}(D)$ in the high-density branch of Helium. The predicted threshold remains unchanged, provided radiation won't be significantly higher in Helium plasmas compared to Hydrogen plasmas in ITER.

We now turn to the Hydrogen and Helium data points circled in black in Fig. 4a and 4b, with 1.2 MA, 1.8 T, instead of the 1.7 MA plasma current of the rest of the data presented in that figure. The Helium point illustrates that, like in D and H, at low density the power threshold drops when the plasma current drops, shifting $\bar{n}_{e,min}$ to lower values [18, 24, 1]. Further, for 1.2MA we can compare D-NBI and RF heating: P_{sep} is the same in Helium for both, but not so P_{loss}, since radiation is quite high for the RF heated Helium plasma at low density. Note that for these low current points the upper axis f_{GW} values of Fig. 4 don't apply.

3.2. Helium plasma simulations with HESEL

The HESEL code [25,26] was applied to investigate the L-H transition in a pure Helium plasma JET#93870 with an L-H transition at 15.45 s and $n_{e,av}=4 \ 10^{19}$ m^{-3}, comparing it with a Deuterium pulse of similar high density. HESEL is a four-field (Vorticity, Density, Ion, and Electron pressures), energy-conserving, drift-fluid model based on the Braginskii equations, describing interchange-driven, low-frequency turbulence in a plane perpendicular to the magnetic field at the outboard mid-plane of a Tokamak plasma. It includes the transition from the confined region to the SOL and the full development of the profiles across the LCFS.

Experimental parameters and edge profiles of electron temperature and electron density just before the LH transition are used as the initial condition. The increasing energy input to the ions is modelled by artificially increasing the ion temperature at the inner boundary of the computational domain *throughout* the simulation. Thermal coupling between electrons and ions is included in the model, but it is found to play only a minor role in the dynamics. Since a plasma of doubly
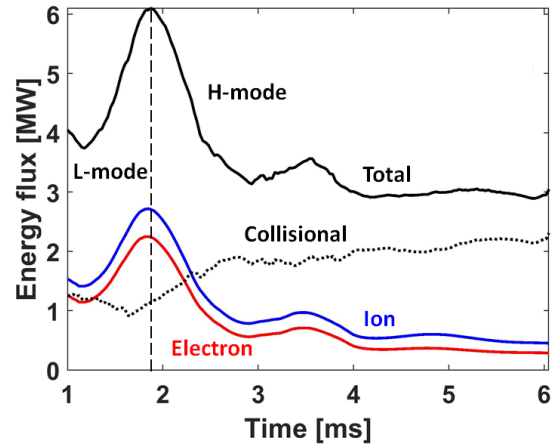

Fig. 5: Energy fluxes across the separatrix as a function of time: electron and ion turbulent fluxes, the collisionality driven energy flux and the total flux. The L-H transition time is marked with a vertical dashed line.

ionized ^{4}He has $n_i=n_e/2$, greater T_i is needed to reach a comparable ∇p_i to trigger a transition. The resulting evolution is displayed in Fig. 5, where we show the evolution of the energy fluxes across the last closed flux surface. The initial phase 0<t<1is dominated by transient adjustments and it is not plotted. The figure shows the full (conductive and convective) turbulent heat fluxes for electrons (red) and ions (blue), due to the fluctuations. The dotted line depicts the collisionality driven heat flux (neoclassical), and the black line shows the sum of all these components. Early on the turbulent fluxes increase due to the forced increase in ion temperature gradient. We observe a transition from an L-mode to H-mode-like confinement at the time marked with a vertical dashed line, when $T_i \sim 3 \times T_e$ at the LCFS. At that time there is a significant reduction of the turbulent transport of energy across the last closed flux surface, both for ions and electrons, even though the ion temperature gradient rise is still being imposed. The power threshold was in the same range as the one for a similar Deuterium plasma corresponding to JET#90993, with $T_i \sim 1.5 \ T_e$ at the LCFS [27]. The neoclassical collisional transport (proportional to Z^2, where Z is the charge) for the Helium case is significant when compared with the turbulent transport, especially after the transition, when the turbulent fluxes are lower. In hindsight this is not unexpected, due to the Z^2 dependency of collisionality. Earlier simulations for Hydrogen isotopes [27] found collisional

Recent progress in L–H transition studies at JET tritium, helium, hydrogen and deuterium

[Left hand page running head is author's name in Times New Roman 8 point bold capitals, centred. For more than two authors, write **AUTHOR et al.**]

transport to be much smaller than the turbulent transport, both before and after the L-H transitions. The model shows that the improvement in confinement after the L-H transition is less notable in Helium than in Hydrogenic species due to the larger contribution of the collisional fluxes in Helium plasmas.

3.3. ELMs in Helium plasmas

In Hydrogen and Deuterium plasmas, with sufficient NBI heating, it is common to observe the coherent M-mode [9] at the L-H transition. As input power increases small ELMs appear mixed with the M-mode, until eventually isolated ELMs appear, often described as Type I ELMs. The same pattern is observed in Helium plasmas, as shown in Fig. 6. The pulse shown in Fig. 6 is the 1.2 MA Helium D-NBI heated data point of Figs. 4a and 4b, marked in those figures with hollow triangles circled in black. Entry into H-mode took place at $n_{e,av}=2.8\times10^{19}$ m^{-3} with $P_{sep}= 2.8$ MW. During the ELMy H-mode, the average density rose slightly to 3.2×10^{19} m^{-3}, even though He gas fuelling was turned off by the density feedback system as soon as the plasma entered H-mode. Eventually the plasma displays well separated large ELMs. The P_{sep} required to reach these "large" ELMs in Helium is of order 5 MW. It was not possible to
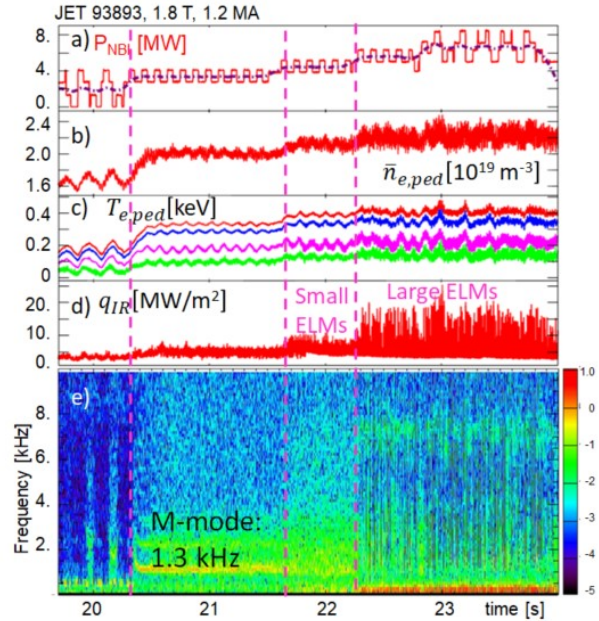

Fig. 6: ELMs in Helium D-NBI heated plasma. a) NBI input power, measured and smoothed; b) $n_{e,ped}$; c) $T_{e,ped}$; d)IR-measure heat flux at outer target; e) spectrogram of inboard Mirnov signal (log scale colour contours), showing M-mode and quiet periods in between ELMs
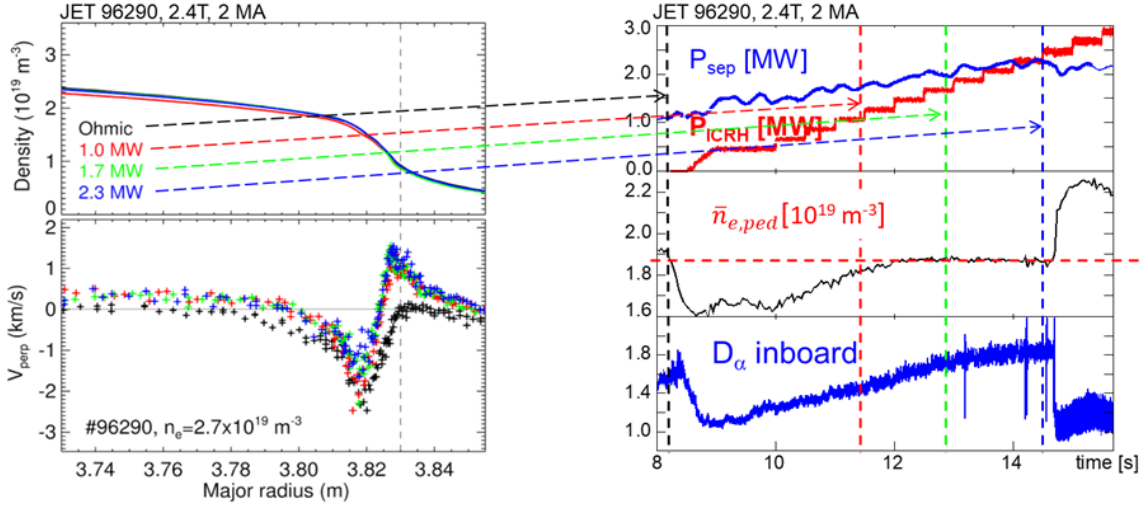
document an increase in ELM frequency as power increases. The high natural ELM frequency, of order 100 Hz, and low $T_{e,ped}<0.5$ keV, imply that ELM pacing techniques such as kicks or pellets (technically limited to lower frequencies at JET) can't be tested in these Helium plasmas.

The estimated drop in plasma electron energy per ELM is 30-40 kJ, compared to 130 kJ electron pedestal energy. This is high, but comparable to similar ELMs in Deuterium. An MHD stability analysis of peeling-ballooning modes, assuming $T_i=T_e$, finds **stable** conditions just before the ELM, as is often the case in high-density plasmas in JET-ILW [28,29]. We can't identify these ELMs conclusively as type I or type III. The very limited duration of this Helium campaign didn't allow further investigation of ELMs in Helium.

4. L-H TRANSITION STUDIES IN DEUTERIUM

4.1. Evolution of edge radial electric field along power ramp

Measurements of the propagation velocity of edge fluctuations, $v_\perp= v_{E\times B}+v_{phase}$, can be obtained at JET with Doppler Reflectometry [30, 31]. Typically in the edge v_{phase} is ignorable and $v_\perp$ is a good proxy for the radial electric field. To localise the measurement, accurate electron density profiles are necessary. The density profiles from the profile reflectometer [32] were calculated from the time-of-flight, extracted from spectrograms stacked from 10 probing frequency sweeps [33].

A detailed comparative study of the pre-transition $v_\perp$ profiles across electron density scans in Deuterium and Helium plasmas is presented in [7]. Here we discuss one of the most interesting results: the evolution of the $v_\perp$ profile along the power ramp characteristic of L-H transition studies.

In Fig. 7, on the left, we present electron density and $v_\perp$ profiles taken along a heating ramp used to induce the L–H transition in a 2.4 T 2 MA RF-heated Deuterium plasma in the low-density branch. On the right hand side we show the temporal evolution of the RF power ramp. Initially, as the plasma enters L-mode, the pedestal density drops. This is then compensated by the gas puff system. The initial density value is recovered during the L-mode, up until the transition. The L-H transition time is obvious in rise of $n_{e,ped}$ and the drop of D_α

Recent progress in L–H transition studies at JET: tritium, helium, hydrogen and deuterium

[Left hand page running head is author's name in Times New Roman 8 point bold capitals, centred. For more than two authors, write AUTHOR et al.]

Fig. 7, left: Radial profiles of a) density and b) $v_\perp$ for Deuterium plasmas at different ICRH power levels ($\bar{n}_e = 2.7 \times 10^{19}$ m^{-3}). The separatrix (dashed line) is at 3.83 (± 0.01) meters. (Reproduced from Silva et al [7], with permission)
Fig. 7 right: temporal evolution of a) P_{sep}, RF heating; b) line averaged pedestal density; c) Inboard D_α

at 14.69 s. The RF heating ramp was designed to be especially slow to allow acquisition of a full profile of Doppler reflectometry (it takes 308 ms) within each power step. The vertical dashed lines on Fig 7 mark the end of each 308 ms time interval used to produce the profiles shown on the left, the arrows connect profiles and times. Depicted are the steps at 1, 1.7 and 2.3 MW, with very similar density profiles. The SOL flow is observed to increase when the auxiliary heating is applied but then exhibits no variation with applied ICRH power up to the transition. The L-H transition takes place 200 ms later when 2.5 MW of heating is applied.

Interestingly, no significant change in the $v_\perp$ profile is observed during the power ramp preceding the L–H transition at the various ICRH power steps. On the other hand, an analysis of the edge kinetic profiles indicates that there is increase of edge ∇p (diamagnetism) along the power ramp [7]. We cannot probe faster time-scales, or edge rotation measurements in this dataset.

Similar behavior was reported in JET NBI-heated plasmas vertical target plasmas [34]: a significant difference in $v_\perp$ profiles was observed between Ohmic and L-mode phases, but also no change was observed during the heating ramp in L-mode.

Our data suggests that the apparent critical inner E_r (or its shear) in Deuterium, discussed in AUG [35], or a critical $E\times B$ velocity [36] before the L-H transition could in fact be a characteristic of L-mode plasmas, at any distance from the L-H transition. The fact that no variation is observed in $v_\perp$ shear (inner or outer), and that if anything the $v_\perp$ well becomes shallower as the transition is approached, appears to indicate that a (time-averaged) critical mean E_r profile or its shear do not provide the trigger for the L-H transition. Similar phenomenology was already described in JET-C [37], with E_r profiles obtained from impurity charge exchange measurements. A clear and sudden change of E_r, as well as many other variables, is described between before and after L-H transitions.

More details and other L-H transitions in He and D plasmas have been studied with Doppler reflectometry, and they are presented in [6]. We chose to highlight this particular result here because it signals a departure from conventional ideas.

4.2. Ion heat flux analysis near $\bar{n}_{e,min}$: 3 T, 2.5 MA

L-H transitions in Deuterium plasmas at high field, 3 T, 2.5 MA, were obtained to optimise threshold measurements. NBI heating ramps were used to obtain ion temperature (T_i) measurements of the main ion species [38], to ensure the power threshold was not modified by injected impurities, which are usually needed for CX measurements in JET-ILW [20]. Experimental profiles of density and temperatures were used to calculate heating deposition profiles and fast ion losses. P_{loss} and P_{sep} values are shown as a function of density in Fig. 8, a clear minimum is observed in both, although P_{sep} at the lowest density may be underestimated (that is a sawtooth triggered transition). As usual, their error bars are estimated to be of order 10%.

Recent progress in L–H transition studies at JET: tritium, helium, hydrogen and deuterium

[Left hand page running head is author's name in Times New Roman 8 point bold capitals, centred. For more than two authors, write AUTHOR et al.]

A detailed transport analysis was carried out for this set of JET-ILW NBI-heated Deuterium pulses to investigate the possible relationship between the edge ion heat flux at the L-H transition and $\bar{n}_{e,min}$ [39].

In all cases, we found experimentally that $T_e > T_i$ in the plasma core. Although direct NBI ion heating and significant electron to ion exchange power resulted in a larger power coupled to plasma ions than to electrons, ion energy transport is shown to be dominant by gyrokinetic transport simulations, explaining the observed core $T_e > T_i$.

Like the power threshold, P_{loss} or P_{sep}, the edge ion heat flux at the L-H transition, also shown in Fig. 8, exhibits non-linear behaviour as a function of density. A linear trend of the critical edge ion heat flux would have been expected if the ion heat flux dominated the threshold, as in the wave-heated AUG [14] and C-mod discharges [40]. Instead NBI pulses both for JET, shown here [39] and also for AUG, shown in [14], deviate from linearity. Whether this is due to the role of NBI torque on the power threshold, as described in DIII-D [21] is still unclear.
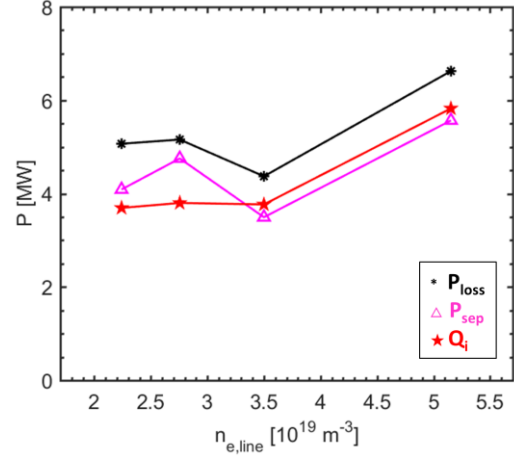

Fig. 8: Power terms at the L-H transition for a set of JET-ILW Deuterium, NBI-heated pulses. P_{loss} is shown with black asterisks, P_{sep} with magenta triangles, edge ion heat flux Q_i with red stars

4.3. L-H transition scaling laws in Deuterium

A database of L-H transitions in Deuterium in the JET-ILW has been assembled as part of the ITPA TC-26 [41]. It contains 107 L-H transitions in a variety of plasma shapes, currents and fields.

Table I lists the $\bar{n}_{e,min}$ values of each dataset/shape. HT-R and HT-L are versions of the HT shape (see Fig. 1) with the outer strike line shifted outward and inward relative to HT, respectively. Only data above the densities quoted on the table was fitted for each plasma configuration. The various shapes and their impact on P_{LH} were described in [1, 2, 3].

Table I

B_{tor} (T)	I_p (MA)	Shape	$\bar{n}_{e,min}$
1.8	1.7	HT	2.2±0.3
1.8	1.7	HT	2.2±0.3
2.4	2.0	HT	2.85±0.1
2.4	2.0	HT-L	2.7±0.2
2.4	2.0	VT	< 2.0
2.4	1.5	HT-high δ	2.2±0.1
3.0	2.75	HT-R	3.3±0.2
3.0	2.5	VT	2.3±0.2
3-3.4	various	CC	2.5±0.2

Table I: $\bar{n}_{e,min}$ as a function of B_t, I_p and shape in the JET-ILW Deuterium database

The ITPA 2008 scaling law [5] is the starting point. The conventional fitting variables are the line averaged density in units of 10^{20} m^{-3}, n_{e20}, the toroidal field B_T in T and the plasma surface area S in m^2:

$$P_{LH} = (0.0488 \pm 0.006) \, n_{e20}^{0.717 \pm 0.035} \, B_T^{0.803 \pm 0.032} \, S^{0.941 \pm 0.019} \qquad (4.1)$$

Fig. 9a displays the new data vs. the ITPA 2008 scaling law, showing the clear impact of shape on the power threshold: HT data points have a lower threshold than the 1:1 line, while CC and VT have higher thresholds. The grey points are from JET-C.

A fit with a similar functional form, but assuming S^l, is sought for P_{loss} in the high density branch, assuming 10% uncertainties. It is found that the data naturally falls in one of two branches: the power threshold is lower for the HT configurations, with the outer strike line on the tilted target, and higher for VT and CC, when the strike lines hit vertical targets or the corners of the divertor. It is possible to develop separate scaling laws for each combined dataset:
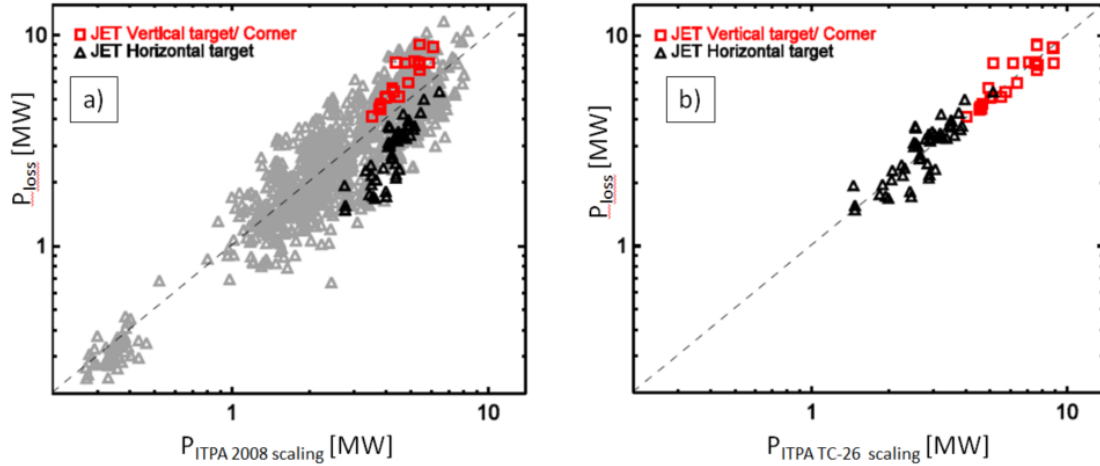
Recent progress in L–H transition studies at JET: tritium, helium, hydrogen and deuterium
[Left hand page running head is author's name in Times New Roman 8 point bold capitals, centred. For more than two authors, write
AUTHOR et al.]

Fig 9a): P_{loss} data vs ITPA 2008 scaling, equation (4.1),   9b) P_{loss} data vs TC-26 2017 scaling, equation (4.4).

$$P_{L-H}(HT) =   (0.057\pm0.012) \, n_{e20}^{1.43\pm0.10} \, B_T^{0.77\pm0.015} \, S^1, \qquad RMSE=17\% \qquad (4.2)$$

$$P_{L-H}(VT/CC) = (0.031\pm0.013) \, n_{e20}^{0.77\pm0.20} \, B_T^{1.29\pm0.24} \, S^1, \qquad RMSE= 10\% \qquad (4.3)$$

Here we note that the sum of density and field coefficients is similar in both cases, with stronger density dependence for the HT shape. Combining both datasets with a simple factor to account for the difference in power threshold due to plasma shape, we obtain a single scaling law with hardly any change of relative RMSE:

$$P_{L-H}= D \, (0.046\pm0.009) \, n_{e20}^{1.31\pm0.09} \, B_T^{0.85\pm0.13} \, S^1, \qquad RMSE= 16\% \qquad (4.4)$$
with D=1.0 for HT,HT-R and HT-L and D=2.06 +/- 0.07 for VT/CC

This scaling law is plotted in Fig. 9 b. The density scaling coefficient has increased relative to ITPA 2008, largely due to the HT dataset.

The reason for the very strong shape dependence of the power threshold in JET-ILW remains unknown, despite edge modelling and additional experimental studies with intermediate shapes.

5.   SUMMARY, DISCUSSION AND OUTLOOK

Recent L-H transition studies at JET have obtained novel results for the dependence of the L-H transition power threshold on plasma ion species.

An NBI-heated Tritium pulse displays lower power threshold than the one inferred from the Deuterium dataset, while ohmic transitions were observed in Tritium plasmas at low density. At the moment we lack the Deuterium references at high density, or NBI heated Tritium at low density, which would be necessary to quantify the impact of ion mass on the L-H threshold.

The Helium power threshold results indicate that access to H-mode in the PFPO phase of the ITER Research Plan may be easier in Helium than in Hydrogen at higher densities. Still, the He H-mode threshold power itself is comparable to D and, not 40% higher as previously assumed, compensating the increase in required power to access the H-mode in Helium at higher densities and providing the same expected threshold.

Modelling shows that heat transport is quite different in Helium plasmas compared to Hydrogen plasmas, with a large collisional contribution both in L and H-mode. Isolated "large" ELMs with frequencies of order 100 Hz, are observed in Helium plasmas with NBI heating, with about twice the heating power required for the transition.

Novel Doppler reflectometry measurements in RF-heated Deuterium plasmas challenge the common assumption that the radial electric field shear builds up along the power ramp until a critical value stabilises turbulence and triggers the transition. This opens up the possibility that alternative explanations for edge transport barrier formation might be applicable, e.g. diamagnetic effects [42, 43], as also pointed out for the transition to Internal Transport barriers [44]. In particular, electromagnetic effects could play a significant role as it happens in core plasmas when diamagnetic effects are important [45]. Actually, even if beta is relative low in L-mode edge plasmas, electromagnetic effects have been shown to play a strong role to explain differences in edge transport for H vs D plasmas in JET [46]. Strong electromagnetic effects would explain the insensitivity to ExB shearing as it has been shown that in plasmas with transport strongly reduced by finite beta the ExB shearing is no longer stabilizing [47]. This will be analysed in the future.

Recent progress in L–H transition studies at JET in tritium, helium, hydrogen and deuterium
[Left hand page running head is author's name in Times New Roman 8 point bold capitals, centred. For more than two authors, write
AUTHOR et al.]

Transport analysis of NBI heated Deuterium plasmas near $\bar{n}_{e,min}$ finds the ion heat flux departs from a linear dependency in n_e as density decreases.

Scaling laws for the L-H transition power threshold in the JET-ILW (restricted to the high-density branch) have been derived, accounting for shape dependency.

The results presented in this paper contribute to advance understanding of the L-H transition and improve the predictive capability towards operation in ITER and future tokamaks.

ACKNOWLEDGEMENTS

REFERENCES

[1]   CF Maggi et al 2014 Nucl. Fusion 54 023007

[2]   E Delabie, "Overview and Interpretation of L-H Threshold Experiments on JET with the ITER-like Wall" [EX-P5] paper presented at 25th IAEA Int. Conf. on Fusion Energy St Petersburg 2014

[3]   J Hillesheim et al, "Role of Stationary Zonal Flows and Momentum Transport for L-H Transitions in JET" Preprint: 2018 IAEA Fusion Energy Conference, Gandhinagar [EX/5-2]

[4]   J Hillesheim et al "Implications of JET-ILW L-H Transition Studies for ITER" Preprint 2018 IAEA Fusion Energy Conference, Gandhinagar. [EX/4-1]

[5]   Y. Martin, et al 2008 J. Phys.: Conf. Ser. 123 012033

[6]   E.R. Solano et al, Nucl. Fusion 61 124001 (2021)

[7]   C Silva et al 2021 Nucl. Fusion 61 126006, https://doi.org/10.1088/1741-4326/ac2abb

[8]   E.R. Solano et al, "L-H Transition Studies at JET: H, D, He and T", Preprint submitted: 2020 IAEA Fusion Energy Conference, Nice (2021) [EX /2-3]

[9]   E.R. Solano et al, Nuclear Fusion, 57, 022021 (2017)

[10] U. Kruezi et al 2020 JINST 15 C01032

[11] S Vartanian, E Delabie, CC Klepper, et al, Fusion Engineering and Design, Vol. 170, p. 112511 (2021)

[12] J.P.H.E. Ongena, Fusion Science and Technology; v. 45; p. 371-379, 2012

[13] Ž. Štancar, Proc. of the 47th EPS Conference on Plasma Physics (21 - 25 June 2021), poster P5.1078 http://ocs.ciemat.es/EPS2021PAP/pdf/P5.1078.pdf

[14] F Ryter et al, Nucl. Fusion 54 083003 (2014)

[15] ITER Research Plan within Staged Approach, ITR-Report 18-003 (2018) p 351

[16] D McDonald et al, *Plasma Phys. Control. Fusion* 46 519 (2004)

[17] P. Gohil et al, Nucl. Fusion 51 (2011) 10

[18] F Ryter et al Nucl. Fusion 53 113003 (2013)

[19] C.E. Kessel et al 2018 Nucl. Fusion 58 056007

[20] S. Menmuir et al., Review of Scientific Instruments 85, 11E412 (2014)

[21] P. Gohil et al 2010 Nucl. Fusion 50 064011

[22] U. Plank et al 2020 Nucl. Fusion 60 074001

[23] JC Hillesheim, 44th EPS Conference on Plasma Physics, 26 - 30 June 2017, Belfast, Northern Ireland (UK), Poster P5.162, (2017) http://ocs.ciemat.es/EPS2017PAP/pdf/P5.162.pdf

[24] Y. Andrew et al Plasma Phys. Control. Fusion 48 479 (2006)

[25] J. Juul Rasmussen et al., (2016), Plasma Phys. Contr. Fusion, 58, 014031

[26] A.H. Nielsen et al., (2015), Physics Letters A, 379, 3097

[27] A.H. Nielsen et al. Invited talk "Numerical investigation of the Low- to High-confinement power threshold for different isotopes of hydrogen and helium at JET", 29th International Toki Conference on Plasma and Fusion Research, Japan, 2020

[28] CF Maggi Nucl. Fusion 55 (2015) 113031

[29] L. Frassinetti et al 2021 Nucl. Fusion 61 126054

Recent progress in L–H transition studies at JET: tritium, helium, hydrogen and deuterium
[Left hand page running head is author's name in Times New Roman 8 point bold capitals, centred. For more than two authors, write
AUTHOR et al.]

[30] J.C. Hillesheim et al., Proc. 12th Inter. Reflectometry Workshop, IRW12

[31] C. Silva et al., Nucl. Fusion 56 (2016) 106026

[32] A. Sirinelli et al., Review of Scientific Instruments 81, 10D939 (2010)

[33] P. Varela et al, Nucl. Fusion 46 S693 (2006)

[34] J. C. Hillesheim, Phys. Rev. Lett. 116, 065002, https://doi.org/10.1103/PhysRevLett.116.065002

[35] M Cavedon, 46th EPS Conference on Plasma Physics, Milano, Italy (2019), poster P5.1069

[36] M. Cavedon et al Nucl. Fusion 60 066026 (2020)

[37] Y. Andrew, European Phys. Letters, 83, 15003 (2008)

[38] E. Delabie et al, "Main ion charge exchange spectroscopy on JET-ILW", 23rd Topical Conference on High-Temperature Plasma Diagnostics, Santa Fe, United States, 14-17 December 2020
https://custom.cvent.com/F6288ADDEF3C4A6CBA5358DAE922C966/files/event/316fe078c3894ef5ab725d6bbdf693 34/28f668af904c41928913f6aad60772d9.pdf

[39] P. Vincenzi et al., 46th EPS Conf.on Plasma Physics, P2.1081, Milano, Italy (2019), to be submitted to Nuclear Fusion

[40] M. Schmidtmayr et al 2018 Nucl. Fusion 58 056003]

[41] E. Delabie et al, 'Status of TC-26: L-H/H-L scaling in the presence of Metallic walls', ITPA meeting September 2017

[42] E. R. Solano, Plasma Phys. Control. Fusion 46 L7 (2004)

[43] E. R. Solano & R. D. Hazeltine, Nucl. Fusion 52 114017 (2012)

[44] J. Garcia J. and G. Giruzzi 2010 Phys. Rev. Lett. 104 205003 (2020)

[45] J. Garcia and G. Giruzzi Nuclear Fusion, 53 043023 (2013)

[46] N. Bonanomi et al, Nucl. Fusion 59 126025 (2019)

[47] J. Garcia et al, Nucl. Fusion 55 053007 (2015)